Coloration and Structure of the Wings of Chorinea sylphina Bates

Author: Dushkina, Natalia

Source: The Journal of the Lepidopterists' Society, 71(1) : 1-11

Published By: The Lepidopterists' Society

URL: https://doi.org/10.18473/lepi.v71i1.a2

Journal of the Lepidopterists' Society
71(1), 2017, 1–11

COLORATION AND STRUCTURE OF THE WINGS OF *CHORINEA SYLPHINA* BATES

NATALIA DUSHKINA*

Department of Physics, Millersville University, P.O. Box 1002, Millersville, PA 17551, USA,
*Corresponding author, e-mail: Natalia.Dushkina@millersville.edu

SEMA ERTEN

NanoMM—Nanoengineered Metamaterials Group, Department of Engineering Science and Mechanics,
The Pennsylvania State University, University Park, PA 16802, USA, e-mail: sue123@psu.edu

AND

AKHLESH LAKHTAKIA

NanoMM—Nanoengineered Metamaterials Group, Department of Engineering Science and Mechanics,
The Pennsylvania State University, University Park, PA 16802, USA, e-mail: akhlesh@psu.edu

ABSTRACT. The structure and the origin of transparency of the wings of *Chorinea sylphina*, a species of glasswinged butterflies, were explored using optical microscopy, scanning electron microscopy, UV photography, spectrophotometry, and optical polarimetry. We found that for normally incident light, the clear transparent areas of the forewings and hindwings exhibit significant transmission as well as minuscule reflection throughout the visible regime in the electromagnetic spectrum. We found that the transparency results from the sparsity, the semitransparency, and the upright orientation of single scales on the wing membrane. The red and dark brown colors of the nontransparent areas of the wings have a pigmentary origin. Coherent scattering from the slanted and overlapping lamellae in the scale ridges and diffraction from every scale's longitudinal network of parallel ridges are responsible for blue iridescence and shimmer at large viewing angles. The transparent areas of the wings function as absorbing linear polarizers, due to both the parallel ridges and the almost unidirectional orientation of individual scales on those areas.

Additional key words: butterflies, transmittance, reflectance, anti-reflection, polarization

While biologists associate the colors of living creatures with mate finding and/or camouflage against predators (Hill 2010), engineers and physicists are increasingly attracted to the intense and often iridescent colors displayed by some tropical butterflies, such as of the genus *Morpho*, because of the potential to reproduce those colors with engineered microstructures rather than via pigments (Kinoshita 2008, Saito 2011, Dushkina & Lakhtakia 2013). The production and use of pigments must be reduced, if not eliminated altogether, because these activities release vast amounts of volatile organic compounds into the biosphere (Brown et al. 1990, Yu & Crump 1998, Leung et al. 2005), causing both chronic and acute distress to humans and other life forms (Mølhave 1990, Bailey et al. 2010, Casals-Casas & Desvergne 2011, Nurmatov et al. 2015).

The diversity and origin of the butterflies' bright iridescent coloration have been extensively studied over the last few decades (Vukusic 2006, Berthier 2007, Kinoshita 2008), and applications have been sought for cosmetics, textiles, security paper, and automotive paints (Saito 2011, Dushkina & Lakhtakia 2013, Poncelet et al. 2015). Comprehensive research focused on the detailed structure of single scales and their contribution to the overall colors in a wing (Kinoshita & Yoshioka 2005, Vukusic 2006, Giraldo 2007, Kinoshita 2008), and led to sophisticated bioinspired nanostructures and bioreplication techniques (Huang et al. 2006, Saito et al. 2006, Martin-Palma et al. 2008, Saito et al. 2012, Gupta et al. 2015, Zobl et al. 2016).

Some researchers are now showing interest in the reasons for and the physical mechanisms underlying clear (i.e., colorless) transparency, which is rare among lepidopterans. Among clear-winged butterfly species, examples are *Greta oto* (Hall 1996) and *Pteronymia zerlina* (Bolaños Martinez et al. 2011), both from the family Nymphalidae, tribe Ithomini, as well as *Chorinea sylphina* Bates of the Riodinidae (Bates 1867-68). Studies of their habitat and life style in captivity (i.e., in butterfly houses) as well as in the wild show that the clear transparent wings easily camouflage the butterfly at rest and also protect it in flight from predatory birds (Johnsen 2001).

The clear transparent wings of *G. oto* were the first to be investigated for their structure, due to the remarkably low haze and reflectance over the portion of the electromagnetic spectrum that is visible to humans (Binetti et al. 2009, Siddique et al. 2015). Scanning electron microscopy (SEM) revealed that the

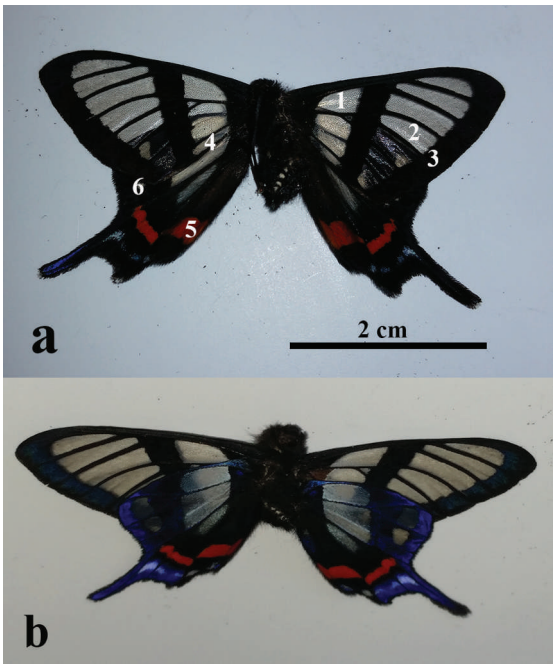

FIG. 1. *Chorinea sylphina*. (**a**) Dorsal view at a small viewing angle. (**b**) Ventral view at a large viewing angle. The investigated areas of the wings are numbered in Fig. 1a as follows: (**1**) inner transparent, (**2**) outer transparent, and (**3**) dark areas of the forewing; (**4**) inner transparent, (**5**) red, and (**6**) outer transparent areas of the hindwing.

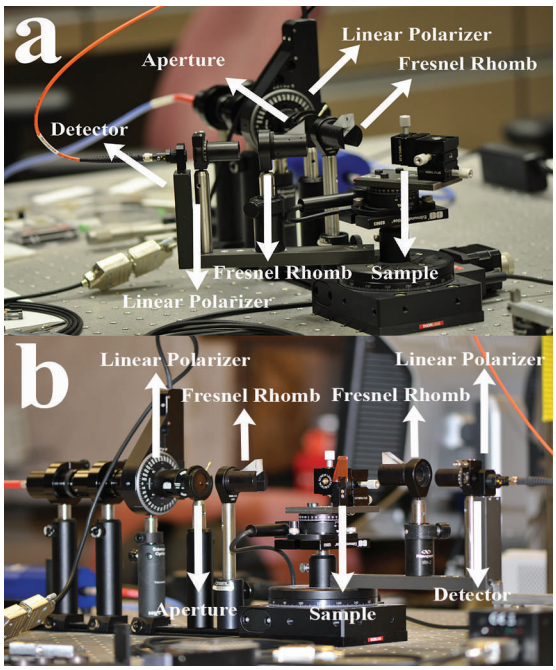

FIG. 2. Variable-angle spectroscopic system configured to measure the (**a**) circular reflectances and (**b**) circular transmittances of a sample. The same configurations but with both Fresnel rhombs removed were used to measure the linear reflectances and linear transmittances.

membrane of any transparent part of a wing is covered by miniature bristles, also called microtrichia, of height and thickness about 2 μm and 40 μm, respectively, and spaced 40–50 μm apart from each other. Similar microtrichia were observed also in other butterflies and were associated with improving the hydrophobicity of the wings (Kristensen & Simonsen 2003, Wanasekara & Chalivendra 2011). Furthermore, SEM analysis revealed the presence of quasi-randomly positioned, high-aspect-ratio nanopillars on the transparent parts, while 2D Fourier power spectra of the top-view SEM images unveiled the random height and width distribution of those nanopillars. Reflection-and-transmission spectrophotometry was used to confirm that this quasi-random nanostructure is responsible for the remarkable broadband and omnidirectional anti-reflection properties of the transparent parts of the wings (Siddique et al. 2015).

An interesting and rare example of a clear-winged butterfly found in Ecuador, Peru, and Bolivia is *Chorinea sylphina* of the Riodinidae family, known also as *sylphina angel*. It was first classified as *Zeonia sylphina* by H. W. Bates in 1867–68 but has been known by its present name after a reclassification that took place earlier than 1910. The *Chorinea* species live in the subtropical broadleaf forests of the Andean mountains at 2000–3000 m altitudes. All four wings of *C. sylphina* have distinctive patterns that feature transparent regions contoured by dark brown, almost black, "veins" and peripheral regions. The other seven existing species in the *Chorinea* genus have clear wings with the same basic pattern as *C. sylphina*, but differ in the configuration and extent of the red/yellow markings on their hindwings. Their beauty is revealed in flight in full sunshine, when the transparent parts of their wings glitter with iridescent green, blue, magenta and golden hues.

The intriguing combination of natural transparency and shimmering colors of the wings of *C. sylphina* drew our attention. Since, to our knowledge, the structure and the origin of the coloration on *C. sylphina* wings seem to have not been studied yet, they became the subject of our investigation reported in this paper.

We used optical and scanning electron microscopy, ultra-violet (UV) photography, spectrophotometry, and polarimetry to analyze the structure and coloration of the wings of *C. sylphina*. Our findings about the *C. sylphina* transparency are compared here with the results for *G. oto* reported by Binetti et al. (2009) and Siddique et al. (2015). In addition, we found that the transparent areas of the *C. sylphina* wings function as UV reflectors and linear polarizers of light.

MATERIALS AND METHODS

Specimen. Ten dead *C. sylphina* specimen were bought from Insect Design (Redbank, QLD, Australia; www.insectdesigns.com). All specimen had red markings on the hindwings. Dorsal and ventral views of the butterfly are shown in Figs. 1a and 1b, respectively. The butterfly has four wings (wingspan of 4.5 cm) with distinct pattern of dark-lined transparent areas on both forewings and hindwings (areas numbered 1, 2, 4 and 6 in Fig. 1a) and red areas on the hindwings (area numbered 5 in Fig. 1a).

Optical Microscopy. The wing structure was observed using (i) an optical microscope (Model 420T-430PHF-10, National Optical Instruments, Schertz, TX, USA) with 10X magnification and (ii) a polarization microscope (Nikon Eclipse LV100D-U, Tokyo, Japan) with objectives Lu Plan Fluor 10X/0.30 (with calibration 0.340 µm/pixel) and Lu Plan Fluor 20X/0.45 (with calibration 0.170 µm/pixel). The samples were observed in epi- and dia- illumination when placed between parallel and crossed polarizers.

Scanning Electron Microscopy. The fine structure of the butterfly wings was studied by a scanning electron microscope (FEI Nova NanoSEM 630, Hillsboro, Oregon, USA). For that purpose, pieces of the different parts of the butterfly wings were processed in a liquid-nitrogen environment and the mounted samples were coated with a gold film of thickness of few nanometers.

Spectrophotometry. The transmittance and reflectance spectra of the transparent areas of the forewings and hindwings of *C. sylphina* were measured with a custom-made spectroscopic system shown in Fig. 2 and described in detail in the Appendix. The spectra were obtained for illumination with unpolarized, linearly polarized, and circularly polarized light. All four linear transmittances (T_{ss}, T_{pp}, T_{sp}, and T_{ps}), linear reflectances (R_{ss}, R_{pp}, R_{sp}, and R_{ps}), circular transmittances transmittances (T_{RR}, T_{LL}, T_{RL}, and T_{LR}), and circular reflectances (R_{RR}, R_{LL}, R_{RL}, and R_{LR}) were measured. Transmittances and reflectances with both subscripts different denote depolarization (Collett 2005, Lakhtakia & Messier 2005).

Polarimetry. Transmission measurements were carried out over the visible regime in the electromagnetic spectrum using a modification of the custom-made spectroscopic system shown in Fig. 2, as described in the Appendix.

RESULTS AND DISCUSSION

Wing anatomy by optical and scanning electron microscopy. Figures 3–5, obtained using optical and scanning electron microscopies, revealed that on both

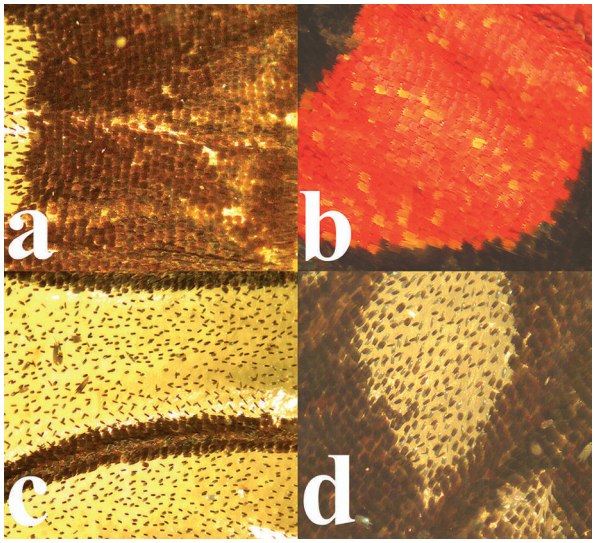

FIG. 3. Photographs of *C. sylphina* wings viewed through an optical microscope (10× magnification). (**a**) Dark area 3 of the forewing, (**b**) red area 5 of the hindwing, (**c**) outer transparent area 2 with black "veins" of the forewing, and (**d**) outer transparent area 6 of the hindwing. The numbered areas are identified in Fig. 1a.

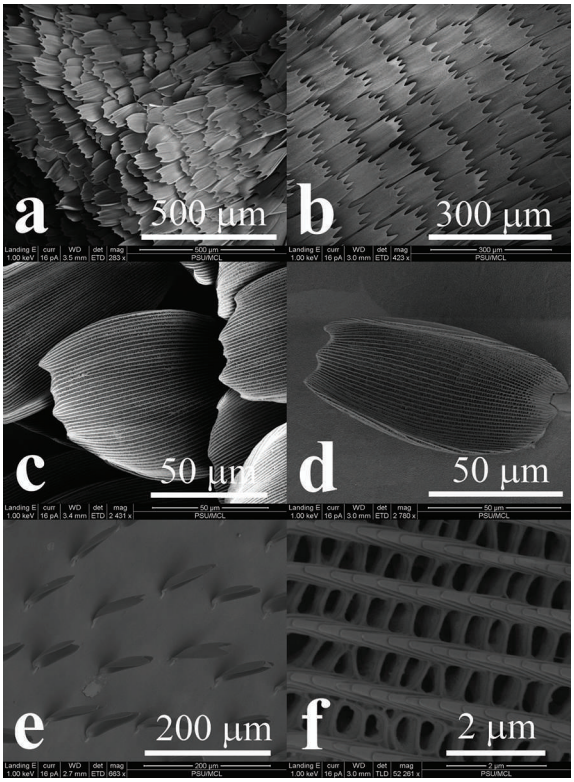

FIG. 4. SEM images of (**a**) the outermost black part of area 3, (b) arrays of scales on the red parts of area 5, (**c**) the black part close to the transparent area 2, (**d**) a single scale on the inner transparent area 4, (**e**) scales on the inner transparent area 1, and (**f**) the microstructure of a scale from the black region of the hindwings. The overlapping lamellae on the ridges function as Bragg mirrors, and the crossribs between adjacent ridges function as diffraction gratings.

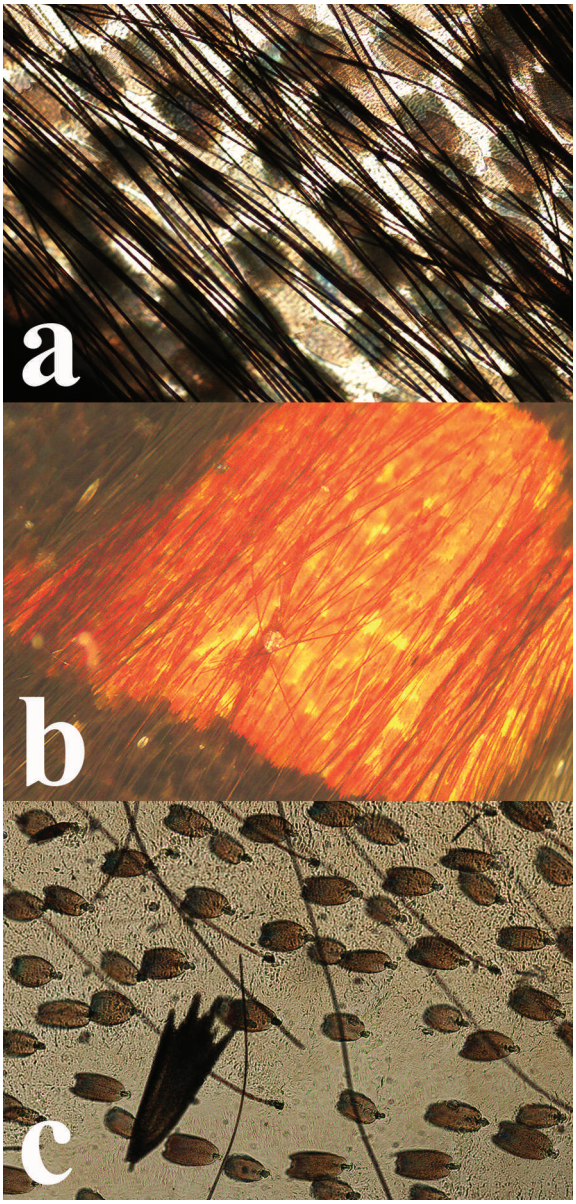

FIG. 5. (**a**) Photograph of hair on the semi-transparent area 6, taken through a polarization microscope with objective Lu Plan Fluor 10x/0.30 and a digital camera; image size 1275×1020 µm. (**b**) 10× magnified photograph of red area 5 taken with an optical microscope. (**c**) Photograph of hair on the large transparent area 4, taken through a polarization microscope with objective Lu Plan Fluor 10x/0.30 and a digital camera; image size 1275×1020 µm.

the ventral and dorsal sides, the wing membrane is covered with flat scales of similar dimensions and microstructure. The inner nontransparent areas, i.e., the dark area 3 (Fig. 3a) and the red area 5 (Figs. 3b and 4b), display nearly perfect arrays of almost identical flat rectangular scales of 127±33 µm length and 79±6 µm width, partially overlapping like shingles on a roof (Fig. 4b). The dark outermost areas of the wings, as well as the veins, are densely covered with loosely stacked rectangular fork-shaped scales (Figs. 3c, 3d, and 4a). In contrast, the scales on the hindwing tails are triangular in shape, with the largest median being 196±8 µm in length, as exemplified by the large scale shown in Fig. 5c. These scale dimensions are typical for Lepidoptera (Ghiradella 1989, 1991; Simonsen & Kristensen 2010) and agree with the dimensions of about 50 µm along the minor axis and 200 µm along the major axis of the brown and white oval scales that cover the nontransparent parts of the *G. oto* wings (Binetti et al. 2009, Siddique et al. 2015).

The wing membrane in the clear transparent areas on both the dorsal and ventral sides of the *C. sylphina* wings is sparsely dusted with semitransparent scales (Figs. 3c and 3d) which do not differ in morphology from the scales that cover the nontransparent black and red areas. Single scales are loosely aligned as checkers on a chessboard, separated by a distance of about 140 µm (about the width of two scales) from their closest neighbors. All scales are aligned in the same direction (Fig. 4e), which is the direction of the black veins, i.e., from the butterfly's body towards the edge of the wings. In the large transparent areas, the single scales bend upward from the glass membrane surface and curl inward along the length of the scale (Figs. 4d and 4e). Therefore, their presence does not impair significantly the visual transparency of the clear areas. Since no structural and dimensional difference were observed between the scales on the clear transparent and the nontransparent areas, one could assume that the scales on the former are the result of evolutionary shredding that left behind a transparent membrane.

The smallest area in the transparent parts of the *C. sylphina* wings that we were able to analyze reliably with SEM was 15×15 µm. At this magnification, we did not observe fine nanopillars. In contrast, nanopillars were seen on the transparent parts of *G. oto*'s wings, but those were imaged with roughly 36 times higher magnification (Siddique et al. 2015). We are planning further investigation by transmission electron microscopy (TEM) and SEM at higher resolution in order to clarify the membrane morphology for *C. sylphina*.

The hindwings of *C. sylphina* are entirely covered with brown hair of cross-sectional thickness about 6 µm and length exceeding 1 mm (Figs. 5a–c). The hair cover both the transparent areas 4 and 6 as well as the black and red areas, and are more densely distributed in the portions of area 6 closer to the dark boundaries than on the central part of area 4 (Fig. 5c). Such hair were not observed on the forewings of *C. sylphina*. The *C. sylphina* hair are longer, thicker, and more densely

distributed than the microtrichia found on the wings of *G. oto* (Binetti et al. 2009, Siddique et al. 2015). Similar microtrichia are also found on the wings of *Actias luna*, a lime-green, nearctic saturniid moth in the family Saturniidae (Wanasekara & Chalivendra 2011). In addition, the *A. luna* microtrichia cover fork-shaped scales similar in shape and size to those on the wings of *C. sylphina*. While the microtrichia in both *G. oto* and *A. luna* are randomly oriented, the much longer and thicker hair on the hindwings of *C. sylphina* are well aligned along the direction of the fork-shaped scales. The presence of microtrichia and hair, respectively, on the scales must cause optical scattering (Bohren & Huffman 1983) and result in the translucence of the wings of *A. luna* and the hindwings of *C. sylphina*.

Morphology of single scales. Single scales from both the clear transparent areas and the colored areas of the *C. sylphina* wings comprise well-defined longitudinal parallel ridges connected by crossribs (Figs. 4d and 4f), as is known for numerous lepidopterans (Ghiradella 1989, 1991). The average distance between adjacent ridges is 1.65±0.04 µm for the scales found in the black areas and 1.42±0.09 µm for the scales found in the transparent areas. The average distance between neighboring crossribs is 0.62±0.02 µm. The crossribs between two adjacent ridges function together as diffraction gratings (Dushkina & Lakhtakia 2013). The ridges are ornamented by partially overlapping lamellae (Fig. 4f). These stacks constitute a multilayered structure which functions as a Bragg mirror (Dushkina & Lakhtakia 2013) to produce interference colors, as becomes clear from Fig. 6a.

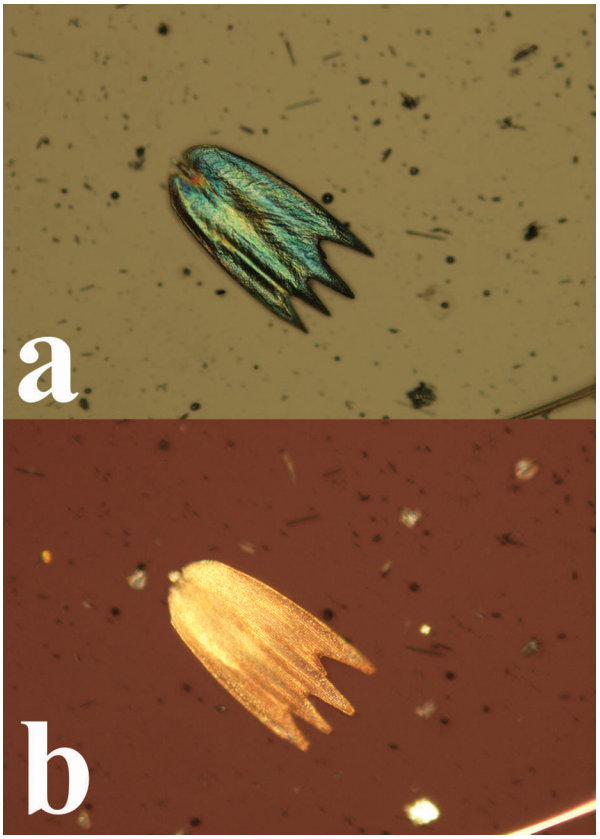

Fig. 6. Color of a single scale from a hindwing of *C. sylphina*, as viewed in epi illumination through a polarization microscope with 20× magnification when the scale was placed between either (**a**) a polarizer and an analyzer with parallel axes of light transmission, or (**b**) two crossed polarizers.

Colors of scales. When viewed in transmitted light, the single scales of *C. sylphina* display a deep brown color indicative of dopamine-derived melanin, a pigment commonly found in lepidopterans (Koch 1995). The scales are semitransparent (Fig. 5c) but, when piled up as in Fig. 4a, produce the darkness of the veins and the outer/peripheral areas of the wings. In the wings of pierid butterflies, pterin pigments are present as granules attached to the crossribs across the scale ridges (Ghiradella 1991, Wijnen et al. 2007, Giraldo & Stavenga 2008). SEM micrographs of the *C. sylphina* wings with four times higher magnification than in Fig. 4f did not show any pigment granules attached to the crossribs. This implies that pigment is distributed throughout the cuticle, which is common in some butterfly families (Allyn & Downey 1977, Stavenga et al. 2004, Wilts et al. 2011).

Yellow, orange, and red colors in many species are of pigmentary origin (Nijhout 1997, Giraldo 2007, Wijnen et al. 2007). For example, xanthopterin and erythropterin produce yellow and orange/red wing coloration by absorbing light in the blue and green portions of the visible regime, respectively (Wijnen et al. 2007). The orange/red coloration of area 5 (Fig. 1a) on the *C. sylphina* wing is also due to the presence of a light-absorbing pigment, as we proved by soaking a hindwing for 3 h in a 5% aqueous solution of sodium bicarbonate ($NaHCO_3$). Within the first half hour of soaking, the red area became milky white and the black areas became light brown.

Erothropterin fluoresces orange/red and is found in butterfly wings. *Vespa orientalis*, a wasp with a large yellow stripe across the body, uses xanthopterin as a light-harvesting pigment to transform solar radiation into electrical energy (Plotkin et al. 2010). Experiments with radiolabelled tryptophan have revealed that red and some brownish pigments are ommochromes such as ommatin (Martel & Laws 1991, Koch 1995). The red bands on the dorsal hindwings of the *Precis coenia* butterfly are almost pure ommatin D, while the orange red marks on the dorsal forewings of the same species are composed of xanthommatin and dihydro-

FIG. 7. Photograph of a wing of *C. sylphina* illuminated with 365-nm UV light.

xanthommatin (Nijhout 1997). The red pigment in area 5 (Fig. 1a) might be one of these pigments, but detailed chemical analysis is necessary for identification.

The black and red areas of the wings of *C. sylphina* exhibit brilliance and shimmer at large viewing angles, an effect which is distinctive for structural colors. The brilliance arises from the orderly arrangement of the scales in the colored areas (Figs. 3a, 3b, and 4b), causing multilayer-interference enhancement of the red color along with diffraction shimmer by the ridges on the scales when viewed at large angles (Dushkina & Lakhtakia 2013).

When bathed in direct sunlight and viewed at large angles, the clear and black areas of the wings of *C. sylphina* shine with a bluish-purplish shimmer (Fig. 1b). The effect is more pronounced in area 4 of the hindwings than on the forewings. However, at normal incidence, the clear parts are highly transparent (Fig. 1a). The play of colors at large viewing angles is typical for structural (i.e., non-pigmental) colors (Dushkina & Lakhtakia 2013) and is due to the ridged morphology of the individual scales (Zhang et al. 2014). The ridged morphology and dimensions of the *C. sylphina* scales are very similar to those of scales of butterflies in the *Morpho* genus (Kinoshita & Yoshioka 2005, Saito 2011) and produce similar bluish iridescence (Fig. 6a). The single scales on the clear areas of the wings of *C. sylphina* are sparsely distributed in a somewhat ordered unidirectional manner creating a pseudo-structure of tiny diffraction gratings. The sunlight glancing on this microstructure is subjected to wavelength-selective coherent scattering from the diffraction micropattern (Berthier 2007, Dushkina & Lakhtakia 2013), thereby producing the brilliant blue reflections.

Some lepidopterans with bright colored wings have scales with UV patterns for attracting mates (Allyn & Downey 1977, Aardema & Scriber 2014). To check the occurrence of that phenomenon in *C. sylphina*, a forewing was illuminated with UV light of wavelength λ_0 = 365 nm from a UV lamp (Model UVGL-25, Mineralight® Lamp multiband UV 254/365 nm, 115V, 60 Hz, 0.16 A). Figure 7 shows strong bluish reflectance from area 1 (Fig. 1a), similarly to the effect reported by Aardema & Scriber (2014).

Reflection and transmission spectrophotometry. Angle-resolved spectroscopy was used to study the optical reflection and transmission characteristics of the clear transparent areas 1, 2, and 4 (Fig. 1a). Figure 8 compares the linear transmittances $T_s = T_{ss} + T_{ps}$ and $T_p = T_{pp} + T_{sp}$ of area 4 for $\lambda_0 \in [400, 900]$ nm, when light hits the sample at an angle $\theta \in [0^o, 70^o]$ with respect to the normal to the plane of the sample. Both T_s and T_p increase gradually and smoothly as λ_0 increases from the UV regime to the near-infrared regime in the electromagnetic spectrum, regardless of the angle of incidence θ. The measured transmittance T_{unpol} for unpolarized incident light displays the same characteristic. The fact that T_p exceeds T_s throughout the whole visible regime indicates an optical-polarization phenomenon discussed later in this section.

Figure 9a compares spectra of the transmittance T_{unpol} of the clear transparent areas 1 and 2 for normally incident ($\theta = 0^o$) unpolarized light. Viewed through an optical microscope, area 2 has fewer scales compared to area 1, which justifies the higher transmittance for area 2. Most likely, the clear transparent areas of the wing membranes of *C. sylphina* are made of α-chitin plus proteins and possibly alkaloids depending on the butterfly's food, just as has been found for *G. oto*, *Godyris duillia*, and *Vanessa cardui* (Binetti et al. 2009). Indeed, the negligible light-absorption characteristics of bulk α-chitin for $\lambda_0 \in [250, 750]$ nm (Azofeifa et al. 2012) are responsible for the uniformly high transmittance of the clear transparent areas in the *G. oto* wings (Binetti et al. 2009).

According to Fig. 9a, the transmittance T_{unpol} of the clear transparent areas of *C. sylphina* wings increases by about 20% through the visible regime wherein bulk α-chitin exhibits negligible light-absorption characteristics (Azofeifa et al. 2012). The adult *C. sylphina* sips nectar from flowers of evergreen plants such as *Prionostemma* spp. (Hippocrataceae) and *Maytenus* spp. (Celastraceae), and migrates up and down mountains to

follow the seasonal changes and the corresponding floral blooms. It is possible that specific alkaloids in the food of *C. sylphina* increase the absorption of light at the blue end of the visible regime, and thereby enhance transmission at the red end of the visible regime. A similar explanation has been proffered for *G. duillia* and *V. cardui* (Binetti et al. 2009). Moreover, light absorption by melanin, the dark brown pigment presumably present in the scales, decreases steadily as λ_0 increases (Riesz 2007), which could also assist in enhancing transmission of red light over blue light.

Figure 9b shows the measured values of the transmittance T_{unpol} of area 4 for $\theta \in \{0^o, 10^o, 20^o, 30^o, 40^o, 50^o, 60^o, 70^o\}$ when λ_0 = 500 nm and the incident light is unpolarized. Also shown in that figure are the values of the sum $(T_s + T_p)/2$ calculated from the standard Fresnel formulas (Born & Wolf 1980) for a 550-nm-thick film (Siddique et al. 2015) of α-chitin of refractive index 1.552 (Leertouwer et al. 2011); the transmittance values from the Fresnel formulas were multiplied by a factor of 0.755 $cos^2\theta$ to account for (i) the absorption and scattering of light from the individual scales sparsely distributed in area 4 and (ii) the elliptical area of illumination of the sample when θ is large. Transparency requires weak absorption, weak reflection, and weak scattering of light. Absorption by melanin and scattering by the single scales distributed sparsely on the clear transparent areas, as well as reflection from the chitin-rich membrane, reduce the transmittance T_{unpol} at normal incidence to about 0.37 for λ_0 = 500 nm (Fig. 9b).

For incident unpolarized light, the measured reflectance of the clear transparent area 1 for $\theta \in \{10^o, 60^o, 70^o\}$ was below 0.01 through the whole visible spectrum. When viewed obliquely at large angles θ in direct sunlight, the dark areas of the wings display the visually intense blue iridescence shown in Fig. 1b. We hoped to detect a blue shift in the reflectance spectrum from the dark parts on increasing θ, but conclusive results were not obtained since the intensity levels of the experimentally obtained reflectance spectra were very small (< 0.004) and quite noisy. The ultralow reflectances of the clear transparent area 1 for a wide range of θ over the entire visible spectrum are in agreement with the 0.02 value of reflectance at $\theta = 65^o$ reported for *G. oto* wings (Siddique et al. 2015).

Spectra of the linear transmittances (T_{pp}, etc.) and linear reflectances (R_{pp}, etc.) of the dorsal transparent parts of the wings of *C. sylphina* were found to be the same, within experimental uncertainty, as those measured of the ventral transparent parts. This result was expected since our optical and SEM investigations showed no morphological differences between the ventral and dorsal transparent areas of the wings of *C. sylphina*.

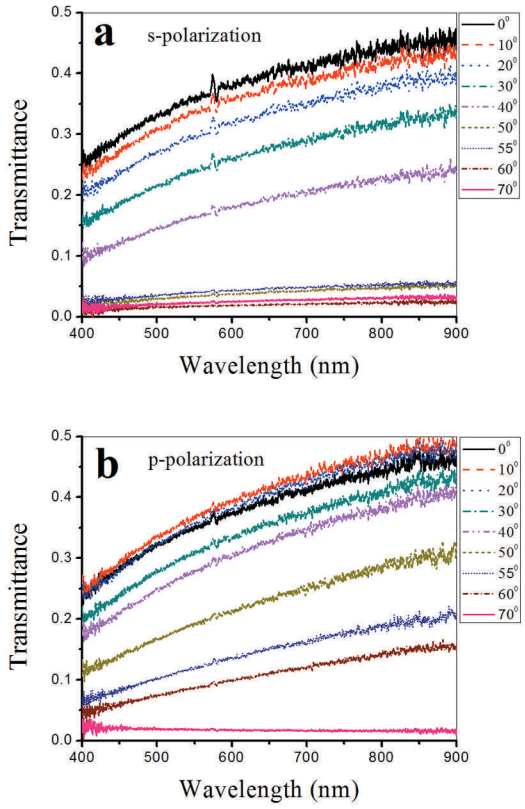

FIG. 8. Measured spectra of the linear transmittances (**a**) $T_s = T_{ss} + T_{ps}$ and (**b**) $T_p = T_{pp} + T_{sp}$ of the clear transparent area 4 for angles of incidence $\theta \in [0^o, 70^o]$.

Optical-polarization phenomenon. Biophotonic structures found on the wing scales of some iridescent beetles (such as *Chrysochroa fulgidissima*) and butterflies (such as *Papilio blumei*) can polarize incident sunlight due to multiple inner reflections from multilayered structures (Berthier 2007, Stavenga et al. 2011). The polarization phenomenon and intrinsic color-mixing properties of bionanostructures are of special interest for anti-counterfeiting measures (Poncelet et al. 2015).

The surfaces of the wing membranes of *G. oto* are decorated with high-aspect-ratio nanopillars, which are responsible for reflection reduction and clear transparency (Binetti et al. 2009, Siddique et al. 2015). However, transmission electron microscopy did not reveal any structural details in the cross-section of the wing membrane, which would imply that no optical-polarization phenomenon is likely to be observed in the *G. oto* wings.

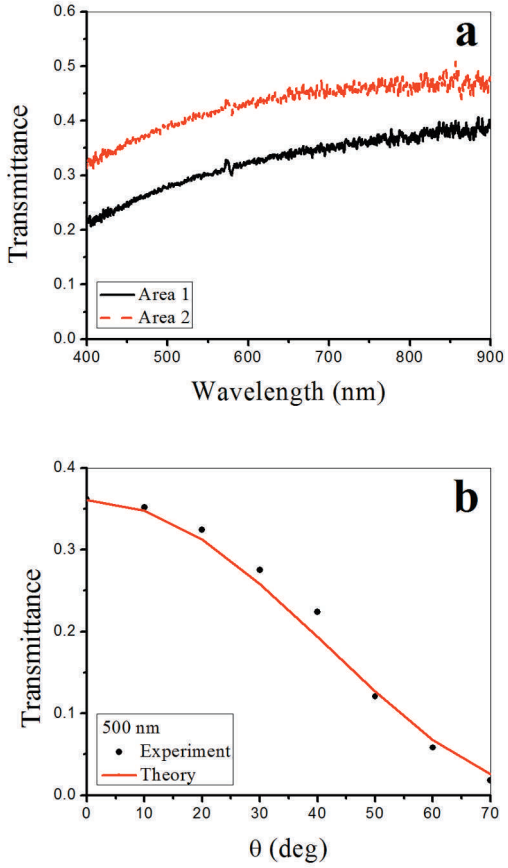

FIG. 9. (**a**) Measured spectra of the transmittance T_{unpol} of the clear transparent areas 1 and 2 for normally incident ($\theta = 0^o$) unpolarized light. (**b**) Circles: measured values of T_{unpol} of area 4 for $\theta \in [0^o, 70^o]$ and $\lambda_0 = 500$ nm, when the incident light is unpolarized. Solid line: predicted values of $(T_s + T_p)/2$ of a 550-nm-thick layer of chitin for $\theta \in [0^o, 70^o]$ and $\lambda_0 = 500$ nm.

In contrast, our studies using a polarization microscope showed that the wings of *C. sylphina* display an optical-polarization phenomenon. In general, polarized colors are produced by materials with periodic variation in refractive index in one or two dimensions. In butterflies, this effect is mainly related to the ridged microstructure of the wing scales (Zhang et al. 2014). In order to produce Fig. 6a, the scale was placed between a polarizer and an analyzer with parallel axes of transmission; the same scale was placed between crossed polarizers in order to produce Fig. 6b. Thus, these two figures show that the intense iridescent color of a single scale is linearly polarized by the periodic array of parallel ridges.

Next, we performed experiments with normally incident ($\theta = 0^o$) circularly polarized light. We found that the circular reflectances (R_{LL}, etc.) were minuscule in magnitude. Furthermore, $T_{LL} = T_{RR}$ and $T_{RL} = T_{LR}$, within experimental uncertainty, for $\lambda_0 \in [400, 900]$ nm. These results were expected since cross-sectional SEM images had not revealed any helical structures (De Silva et al. 2005) in the wing membranes that could discriminate between incident left- and right-circular polarization states (Lakhtakia & Messier 2005).

To further study the optical-polarization effect from the *C. sylphina* wings, we carried out polarimetry experiments (Collet 2005). Measured values of T_{pol} of the transparent area 1 for normally incident ($\theta = 0^o$) linearly polarized light are shown in Fig. 10 as functions of the angle of polarization $\theta_p \in [0^o, 360^o)$ for $\lambda_0 \in \{480, 520, 600\}$ nm, with $\theta_p = 0^o$ corresponding to the *p*-polarization state. Clearly, T_{pol} is an oscillating function of θ_p. As the forewing sample was positioned with the black veins almost parallel to the initial position of the transmission axis of the linear polarizer ($\theta_p = 0^o$) and T_{pol} is maximum at about $\theta_p = 80^o$ for all three wavelengths, the polarization axis of the wing membrane is almost perpendicular to the black veins.

In order to model the experimental data in Fig. 10, we adopted the following methodology. When unpolarized light is incident upon two ideal linear polarizers with transmission axes at an angle θ_p, the irradiance *I* transmitted through the second polarizer is given by Malus' law $I = I_0 \cos^2 \theta_p$, where I_0 is the irradiance of the incident unpolarized light (Born & Wolf 1997). In our polarimetry experiments, the transparent wing membrane, playing the role of a second polarizer, served as an analyzer. In addition, the measured values of T_{pol} were normalized with the irradiance measured after the first polarizer, i.e., *p*-polarized light (not the irradiance of the incident unpolarized light). To account for this and also for the fact that the wing membrane is not an ideal polarizer, the experimental data in Fig. 10 were fitted to the modification

$$T_{pol} = T_o \cos^2(\theta_p) + T_b \quad (1)$$

of Malus' law, where T_b represents the transmittance of the wing membrane which is not influenced by the state of polarization of the incident light and T_0 is the amplitude of modulation due to the wing's optical polarization characteristics. The experimental data were fitted with $T_0 = 0.029$ for all three wavelengths, and $T_b = 0.3$, 0.33, and 0.37 for $\lambda_0 = 480$, 520, and 600 nm, respectively. The differences between the experimental data and the corresponding solid curve for the same value of λ_0 in Fig. 10 indicates that the transparent wing membrane has an optical role additional to that of a polarizer.

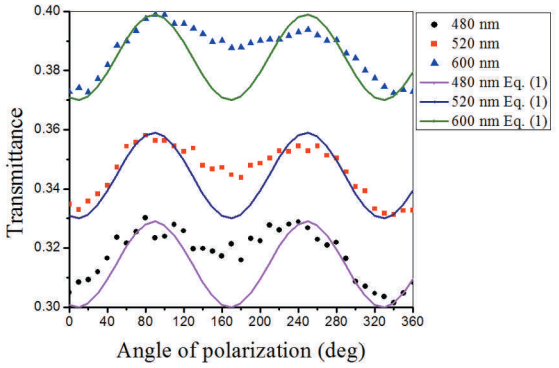

FIG. 10. Transmittance T_{pol} of area 1 measured as a function of the angle of polarization θ_p for normally incident linearly polarized light.

In conclusion, we have investigated the morphology of the wings of the glass-winged butterfly *C. sylphina* to determine the origin of transparency. Spectrophotometry experiments showed that a minuscule fraction of the intensity of normally incident light is reflected whereas about 40% of the intensity of normally incident light is transmitted by the clear transparent areas in the wings, over the entire visible regime. This transparency is a result of: (1) the sparse distribution of single scales on the wing membrane, (2) the semitransparency of the individual scales, and (3) the upright orientation of the scales that leaves much of the wing membrane uncovered. It is possible that a large number of scales fell off the transparent areas of the wings during eclosion. The red and dark brown colors of the nontransparent areas of the wings arise from pigments. The scales' blue iridescence and shimmer at large viewing angles result from coherent scattering from the slanted and overlapping lamellae in the scale ridges and the diffraction from every scale's longitudinal network of parallel ridges. Polarimetry experiments showed that the transparent areas of the wings function partially as linear polarizers, due to both the parallel ridges and the almost unidirectional orientation of individual scales on those areas. The same areas also function as partial absorbers of incident light. Further studies with transmission electron microscopy and analytical chemistry are necessary to clarify all the mechanisms of the coloration of the wings of *C. sylphina*.

ACKNOWLEDGEMNTS

We thank Steven E. Swiontek for taking the pictures in Figs. 3 and 5b. ND acknowledges Millersville University for granting her a sabbatical leave, and the Pennsylvania State University for hosting and supporting her sabbatical research. SE thanks the Turkish Ministry of National Education for financial support of her graduate studies. AL is grateful to the Charles Godfrey Binder Endowment at Penn State for ongoing support of his research activities.

LITERATURE CITED

AARDEMA, M. L. & J. M. SCRIBER. 2014. Ultraviolet coloration in tiger swallowtail butterflies (*Papilio glaucus* group, Papilionidae) with a method for objectively quantifying adult butterfly wing wear. J. Lepid. Soc. 69:58–62.

ALLYN JR., A. C. & J. C. DOWNEY. 1977. Observations on male U-V reflectance and scale ultrastructure in *Phoebis* (Pieridae). Bull. Allyn Mus. 42:1–6.

AZOFEIFA, D. E., H. J. ARGUEDAS, & W. E. VARGAS. 2012. Optical properties of chitin and chitosan biopolymers with application to structural color analysis. Opt. Mater. 35:175–183.

BAILEY, H. D., E. MILNE, N. H. DE KLERK, L. FRITSCHI, J. ATTIA, C. COLE, B. K. ARMSTRONG, & AUS-ALL CONSORTIUM. 2011. Exposure to house painting and the use of floor treatments and the risk of childhood acute lymphoblastic leukemia. Int. J. Cancer 128:2405–2414.

BATES, H. W. 1867-68. A catalogue of Erycinidæ, a family of diurnal Lepidoptera. J. Linn. Soc. Lond. Zool. 9:367–459.

BERTHIER, S. 2007. Iridescences: The physical colors of insects. Springer, New York, NY, USA.

BINETTI, V. R., J. D. SCHIFFMAN, O. D. LEAFFER, J. E. SPANIER, & C. L. SCHAUER. 2009. The natural transparency and piezoelectric response of the *Greta oto* butterfly wing. Integr. Biol. 1:324–329.

BOHREN, C. F. & D. R. HUFFMAN. 1983. Absorption and scattering of light by small particles. Wiley, New York, NY, USA.

BOLAÑOS MARTINEZ, I. A., GONZALEZ, G. Z. & K. R. WILLMOTT. 2011 Descripción de los estados inmaduros de *Pteronymia zerlina zerlina, P. zerlina machay, P. veia florea* y *P. medellina* de Colombia y del Ecuador (Lepidoptera: Nymphalidae: Ithomiini). Trop. Lepid. Res. 21:27–33.

BORN, M. & E. WOLF. 1997. Principles of optics, pp. 61–66. Cambridge Univ. Press, Cambridge, United Kingdom.

BROWN, V. M., D. CRUMP & D. GARDINER. 1990. Determination of aromatic hydrocarbon emissions from paint and related products by an impinger method. Environ. Int. 16:283–289.

COLLETT, E. 2005. Field guide to polarization. SPIE Press, Bellingham, WA, USA.

CASALS-CASAS, C. & B. DESVERGNE 2011. Endocrine disruptors: From endocrine to metabolic disruption. Ann. Rev. Physiol. 73:135–162.

DE SILVA, L., I. HODGKINSON, P. MURRAY, Q. H. WU, M. ARNOLD. J. LEADER, & A. MCNAUGHTON. 2005. Natural and nanoengineered chiral reflectors: Structural color of Manuka beetles and titania coatings. Electromagnetics 25:391–408.

DUSHKINA, N. & A. LAKHTAKIA. 2013. Structural colors, pp. 267–303. *In* Lakhtakia, A. & R. J. Martín-Palma (Eds.), Engineered biomimicry. Elsevier, Waltham, MA, USA.

GHIRADELLA, H. 1989. Structure and development of iridescent butterfly scales: Lattices and laminae. J. Morphol. 202:69–88.

GHIRADELLA, H. 1991. Light and color on the wing: structural colors in butterflies and moths. Appl. Opt. 30:3492–3500.

GIRALDO, M. A. 2007. Butterfly wing scales: Pigmentation and structural properties. Ph.D. Thesis, University of Groningen, The Netherlands.

GIRALDO, M. A. & D. G. STAVENGA. 2008. Wing coloration and pigment gradients in scales of pierid butterflies, Arthropod Struct. Dev. 37:118–128.

GUPTA, T., S. E. SWIONTEK, & A. LAKHTAKIA. 2015. Simpler mass production of polymeric visual decoys for the male Emerald Ash Borer (*Agrilus planipennis*). J. Bionic Eng. 12:263–269.

HALL, S. K. 1996 Behaviour and natural history of *Greta oto* in captivity (Lepidoptera: Nymphalidae: Ithomiini). Trop. Lepid. 7:161–165.

HILL, G. E. 2010. Bird coloration. National Geographic, Washington, DC, USA.

HUANG, J., X. WANG, & Z. L. WANG, 2006. Controlled replication of butterfly wings for achieving tunable photonic properties. Nano Lett. 6:2325–2331.

JOHNSEN, S. 2001. Hidden in plain sight: The ecology and physiology of organismal transparency. Biol. Bull. 201:301–318.

KINOSHITA, S. 2008. Structural colors in the realm of nature. World Scientific, Singapore.

KINOSHITA, S. & S. YOSHIOKA. 2005. Structural colors in nature: the role of regularity and irregularity in the structure. Chem. Phys. Chem. 6:1442–1459.

KOCH, P. B. 1995. Colour pattern specific melanin synthesis is controlled by ecdysteroids via dopa decarboxylase in wings of *Precis coenia* (Lepidoptera: Nymphalidae). Eur. J. Entomol. 92:161–167.

KRISTENSEN, N. P. & T. J. SIMONSEN. 2003. 'Hairs' and scales, pp. 9–22. *In* Kristensen, N. P. (Ed.), Handbook of zoology Vol. IV, Part 36, Lepidoptera, moths and butterflies 2: Morphology, physiology and development. Walter de Gruyter, Berlin.

LAKHTAKIA, A. & R.J. MARTIN-PALMA (Eds.). 2013. Engineered biomimicry. Elsevier, Waltham, MA, USA.

LAKHTAKIA, A. & R. MESSIER. 2005. Sculptured thin films: Nanoengineered morphology and optics, pp. 189–190. SPIE Press, Bellingham, WA, USA.

LEERTOUWER, H. L, B. D. WILTS, & D. G. STAVENGA. 2011. Refractive index and dispersion of butterfly chitin and bird keratin measured by polarizing interference microscopy. Opt. Express 19:24061–24066.

LEUNG, M. K. H., C.-H. LIU, & A. H. S. CHAN. 2005. Occupational exposure to volatile organic compounds and mitigation by push-pull local exhaust ventilation in printing plants. J. Occup. Health 47:540–547.

MARTEL, R. R. & J. H. LAW. 1991. Purification and properties of an ommochrome-binding protein from the hemolymph of the tobacco hornworm, *Manduca sexta*. J. Biol. Chem. 266:21392-21398.

MARTÍN-PALMA, R. J., C. G. PANTANO, & A. LAKHTAKIA. 2008. Biomimetalizaion of butterfly wings by the conformal-evaporated-film-by-rotation technique for photonics. Appl. Phys. Lett. 93:083901.

MØLHAVE, L. 1990. Volatile organic compounds, indoor air quality and health. Indoor Air 1:357–376.

NIJHOUT, H. F. 1997. Ommochrome pigmentation of the linea and rosa seasonal forms of *Precis coenia* (Lepidoptera: Nymphalidae). Arch. Insect Biochem. Physiol. 36:215–222.

NURMATOV, U. B., N. TAGIYEVA, S. SEMPLE, G. DEVEREUX & A. SHEIKH. 2014. Volatile organic compounds and risk of asthma and allergy: a systematic review. Eur. Respira. Rev. 24 (135):92–101.

PLOTKIN, M., I. HOD, A. ZABAN, S. A. BODEN, D. M. BAGNALL, D. GALUSHKO, & D. J. BERGMAN. 2010. Solar energy harvesting in the epicuticle of the oriental hornet (*Vespa orientalis*). Naturwissenschaften 97:1067–1076.

PONCELET, O., G. TALLIER, P. SIMONIS, A. CORNET, & L. A. FRANCIS. 2015. Synthesis of bio-inspired multilayer polarizers and their application to anti-counterfeiting. Bioinsp. Biomim. 10:026004.

RIESZ, J. 2007. The spectroscopic properties of melanin. Ph.D. Thesis, University of Queensland, Australia.

SAITO, A. 2011. Material design and structural color inspired by biomimetic approach. Sci. Technol. Adv. Mat. 12:064709.

SAITO, A., Y. MIYAMURA, M. NAKAJIMA, Y. ISHIKAWA, K. SOGO, Y. KUWAHARA, & Y. HIRAI. 2006. Reproduction of the *Morpho* blue by nanocasting lithography. J. Vac. Sci. Technol. B 24:3248–3251.

SAITO, A., J. MURASE, M. YONEZAWA, H. WATANABE, T. SHIBUYA, M. SASAKI, T. NINOMIYA, S. NOGUCHI, M. AKAI-KASAYA, & Y. KUWAHARA. 2012. High-throughput reproduction of the *Morpho* butterfly's specific high contrast blue. Proc. SPIE 8339:83390C.

SIDDIQUE, R. H., G. GOMARD, & H. HÖLSCHER. 2015. The role of random nanostructures for the omnidirectional anti-reflection properties of the glasswing butterfly. Nature Commun. 6:6909.

SIMONSEN, T. J., & N. P. KRISTENSEN. 2010. Scale length/wing length correlation in Lepidoptera (Insecta). J. Nat. Hist. 20:673–679.

STAVENGA, D. G., S. STOWE, K. SIEBKE, J. ZEIL, & K. ARIKAWA. 2004. Butterfly wing colours: scale beads make white pierid wings brighter. Proc. Royal Soc. Lond. B 271:1577–1584.

STAVENGA, D. G., B. D. WILTS, H. L. LEERTOUWER, & T. HARIYAMA. 2011. Polarized iridescence of the multilayered elytra of the Japanese jewel beetle, *Chrysochroa fulgidissima*. Phil. Trans. Royal Soc. Lond. B 366:709–723.

YU, C. & D. CRUMP. 1998. A review of the emission of VOCs from polymeric materials used in buildings. Build. Environ. 33:357–374.

VUKUSIC, P. 2006. Structural colour in Lepidoptera. Curr. Biol. 16:R621–R623.

WANASEKARA, N. D. & V. B. CHALIVENDRA. 2011. Role of surface roughness on wettability and coefficient of restitution in butterfly wings. Soft Matt. 7:373–379.

WIJNEN, B., H. L. LEERTOUWER & D. G. STAVENGA. 2007. Colors and pterin pigmentation of pierid butterfly wings. J. Insect Physiol. 53:1206–1217.

WILTS, B. D., P. PIRIH & D. G. STAVENGA. 2011. Spectral reflectance properties of iridescent pierid butterfly wings. J. Comp. Physiol. A. 197:693–702.

ZHANG, K., Y. TANG, J. MENG, G. WANG, H. ZHOU, T. FAN, & D. ZHANG. 2014. Polarization-sensitive color in butterfly scales: polarization conversion from ridges with reflecting elements. Opt. Express 22:27437–27450.

ZOBL, S., W. SALVENMOSER, T. SCHWERTE, I. C. GEBESHUBER, & M. SCHREINER. 2016. *Morpho peleides* butterfly wing imprints as structural colour stamp. Bioinsp. Biomim. 11:016006.

Submitted for publication 20 April 2016; revised and accepted 1 September 2016.

SEE APPENDIX ON NEXT PAGE

APPENDIX

Spectrophotometry. The transmittance and reflectance spectra of the transparent areas of the wings of *C. sylphina* were measured with a custom-made computer-controlled variable-angle spectroscopic system depicted in Fig. 2. A halogen light source (HL-2000, Ocean Optics, Dunedin, FL, USA) was used to illuminate the sample. For the transmittance measurements, a butterfly wing was mounted on a metal holder with a circular opening. This setting allowed us to obtain various transmittances of the sample directly without using a glass substrate for the sample. The sample was mounted on a rotatable stage that allowed sample positioning in a specific orientation with angular precision of 5 arc minutes. Measurements were obtained from all transparent areas of the forewings and hindwings illuminated with unpolarized, linearly polarized, or circularly polarized light. For illumination with unpolarized light, white light from the halogen source was guided through an optical fiber and made to impinge directly on the sample. For illumination with linearly polarized light, the sample was positioned between two Glan–Taylor linear polarizers. The first polarizer (GT10, ThorLabs, Newton, NJ, USA) was used to select the linear polarization state (either p or s) of the light impinging on the sample. In the s-polarization (p-polarization) state, the electric (magnetic) field vector of the incident light is oriented perpendicular to the plane of incidence. The second polarizer (GT5, ThorLabs) was used as an analyzer and was set so that the exiting light was either p-polarized or s-polarized.

The exiting light was detected using a CCD spectrometer (HRS-BD1-025, Mightex Systems, Pleasanton, CA) for free-space wavelength $\lambda_0 \in [400, 900]$ nm. For normalization, the light intensity received by the CCD camera in the absence of the sample and the second polarizer was used. All four linear transmittances (T_{ss}, T_{pp}, T_{sp}, and T_{ps}) were measured. The first subscript in T_{sp} denotes the s-polarization state of the transmitted light and the second subscript denotes the p-polarization state of the incident light, and similarly for the other three linear transmittances. Thus, transmittances with both subscripts the same are co-polarized transmittances, whereas those with both subscripts different are cross-polarized transmittances. A non-zero cross-polarized transmittance (or reflectance) indicates depolarization of incident light by the sample (Collet 2005; Lakhtakia & Messier 2005). By virtue of the principle of conservation of energy, no reflectance or transmittance can exceed unity, and there is a similar constraint on appropriate sums of reflectances and transmittances (Lakhtakia & Messier 2005).

The experimental setup for illumination with circularly polarized light is shown in Fig. 2a, with two Fresnel rhombs (LMR1, Thorlabs) used right before and after the sample in addition to the two linear polarizers. All four circular reflectances (R_{RR}, R_{LL}, R_{RL}, and R_{LR}) were measured. The first subscript in R_{RL} abbreviation denotes the right-circular polarization (RCP) state of the reflected light and the second subscript denotes the left-circular polarization (LCP) state of the incident light, and similarly for the other three circular reflectances. The intensity of light received by the CCD spectrometer in the absence of the sample and the second polarizer-rhomb combination was used as the reference. The Fresnel rhombs were removed and the linear polarizers were set appropriately to measure the linear reflectances R_{ss}, R_{pp}, R_{sp}, and R_{ps}. All eight reflectances of the clear transparent areas turned out be less than 0.01, indicating extremely weak reflection of light by the clear transparent areas on the wings.

Figure 2b presents the configuration used to measure the circular transmittances T_{RR}, T_{LL}, T_{RL}, and T_{LR}. Appropriate changes were made to measure the linear transmittances T_{ss}, T_{pp}, T_{sp}, and T_{ps}. For unpolarized incident light, no polarizers and Fresnel rhombs were used, and the transmittance T_{unpol} measured by the CCD spectrometer was recorded.

Polarimetry. For polarimeteric measurements, the incident light was polarized, with the intensities of the p- and s-polarized components in the ratio $\cos^2\theta_p$:$\sin^2\theta_p$, where the angle of polarization $\theta_p \in [0^o, 360^o)$ (Collet 2005). The first polarizer was set to select the angle of polarization θ_p, while the second polarizer was absent. Also, neither Fresnel rhomb was present. The CCD spectrometer measured the transmittance T_{pol} as a function of θ_p and λ_0.